

EFFECT OF FRICTION-STIR-WELDING PARAMETERS ON THE WELDING MICROSTRUCTURE AND PROPERTIES OF 5083 AND 7075 ALUMINUM ALLOYS

VPLIV PARAMETROV VRILNO-TRENJSKEGA VARJENJA NA MIKROSTRUKTURO IN LASTNOSTI ALUMINIJEVIH ZLITIN VRSTE 5083 IN 7075

Yu Zhang^{1*}, Guangchao Liu¹, Peng Sun²

¹College of Mechanical Engineering, Shenyang University, Shenyang 110044

²FAW Jiefang Automobile Co., Ltd, Changchun 130000

Prejem rokopisa – received: 2024-12-13; sprejem za objavo – accepted for publication: 2025-04-22

doi:10.17222/mit.2024.1354

In the friction stir welding (FSW) of 5083 aluminum alloy, an increased tool rotation speed at a constant welding speed promotes flash defects but enhances the symmetry of the "basin-like" weld morphology. The nugget zone features dynamically recrystallized equiaxed grains with peak hardness at the weld center (sharply rising under abrupt rotation acceleration), while the thermo-mechanically affected zone (TMAZ) displays a plastic-deformation microstructure. For 7075 aluminum alloy joints, the grain sizes follow TMAZ > base material > nugget zone, where higher rotation speeds coarsen the nugget/TMAZ grains, whereas increased welding speeds refine them. The average weld hardness reaches 86.6 HB, exceeding TMAZ values, with abrupt rotation speed changes triggering significant hardness surges in 5083 welds.

Keywords: Friction stir welding; 5083 Aluminum alloy; 7075 Aluminum alloy; Dynamic recrystallization

Pri vrtilno-mešalnem trenjskem varjenju (FSW; angl.: friction stir welding) Al zlitine tipa 5083 naraščajoča hitrost vrtenja orodja in konstantna hitrost varjenja pospešujeta nastanek napak zaradi brizganja taline toda izboljšuje se simetrija morfologije varjenja zaradi nastanka kotline z bazenčkom taline. Za cono varjenja, ki ima obliko lešnika (angl.: nugget zone) je značilna tvorba dinamično rekristaliziranih enakoosnih kristalnih zrn z najvišjo trdoto na sredini zvara. Ta močno narašča s pospeševanjem hitrosti vrtenja orodja. Za termo-mehansko vplivano cono zvara (TMAZ; angl.: thermo-mechanically affected zone) pa je značilen nastanek plastično deformirane cone. Pri Al zlitini 7075 sledi velikost kristalnih zrn v zvarnem spoju v smeri TMAZ > osnovni material > lešnikasta cona. Višja hitrost rotacije orodja povečuje razmerje velikosti kristalnih zrn lešnikaste cone proti TMAZ, medtem ko jih povečana hitrost varjenja udrobni. Povprečna trdota zvara je 86,6 HB, kar presega vrednosti za trdoto v TMAZ. Nenadne spremembe hitrosti vrtenja orodja povzročijo znatne skoke trdote v zvarih Al zlitine tipa 5083.

Ključne besede: vrtilno-trenjsko varjenje, zlitine na osnovi Al tipa 5083 in 7075, dinamična rekristalizacija

1 INTRODUCTION

Friction stir welding (FSW), as a solid-phase joining technology, has revolutionized the welding landscape of many metallic materials since its invention.¹⁻³ Traditional fusion welding is prone to defects such as porosity and cracks. However, FSW, with its characteristics of low heat input and no molten pool, effectively avoids such problems and is suitable for heat-sensitive materials such as aluminum alloys and magnesium alloys, meeting the lightweight requirements in aerospace and automotive manufacturing. The aim is to explore its principle, process, factors affecting performance, and clarify the current frontiers and limitations. Many scholars have conducted in-depth research on the process parameters of aluminum-alloy friction stir welding. For example, the

friction stir welding of dissimilar materials such as aluminum alloy and magnesium and magnesium alloys, steel, titanium or copper has important application in aerospace, automotive and other fields and can meet the requirements of different components for material performance and connection.⁴⁻⁷ The research of Bobby et al.⁸ focused on the stress corrosion cracking (SCC) susceptibility of friction stir welded AZ31 magnesium alloy sheets. Through experiments and analysis, the SCC behavior of the welded AZ31 magnesium alloy sheets in a specific environment was discussed, providing an important reference for the application of this material in practical engineering to ensure its safety and reliability during use. Woo et al.⁹ focused on the microstructure, texture and residual stress of friction-stir processed AZ31B magnesium alloy. By analyzing the relationships between these characteristics, the microstructure evolution law and mechanical property change mechanism of the alloy after friction-stir processing were deeply understood, providing theoretical support for further optimizing the processing technology and improving material

*Corresponding author's e-mail:
554068663@qq.com (Yu Zhang)



© 2025 The Author(s). Except when otherwise noted, articles in this journal are published under the terms and conditions of the Creative Commons Attribution 4.0 International License (CC BY 4.0).

performance. Commin L et al.¹⁰ discussed the influence of processing parameters on the friction stir welding of AZ31 magnesium alloy rolled sheets. By changing different processing parameters, the microstructure and performance changes of the welded joints were observed, and the influence law of each parameter on the welding quality was determined, providing a reference for selecting the appropriate process parameters in actual production to obtain welded joints with excellent performance. Afrin N et al.¹¹ studied the microstructure and tensile properties of friction-stir-welded AZ31B magnesium alloy. The microstructure characteristics of different regions of the welded joint were analyzed, and the mechanical properties were measured by tensile tests, revealing the internal relationship between the microstructure and tensile properties. Suhuddin U et al.¹² focused on the grain structure evolution during the friction stir welding of AZ31 magnesium alloy. With the help of advanced microscopic analysis techniques, the growth, deformation and recrystallization of grains during the welding process were studied in detail. Zhou L et al.¹³ studied the microstructure and formation mechanism of the stirred zone in Ti–6Al–4V friction stir welds. Through experiments and theoretical analysis, the change law and formation cause of the microstructure of the stirred zone during the friction stir welding of the alloy were revealed, providing an important basis for understanding the mechanism of titanium-alloy friction stir welding. Liu Liang¹⁴ focused on the microstructure and properties of friction-stir-welded joints of 5052/6061 dissimilar thickness aluminum alloy plates. Through experiments and analysis, the microstructure characteristics, mechanical property change laws and the relationship between the two of the welded joints were systematically studied, providing a theoretical basis and technical support for the process optimization and engineering application of this type of aluminum alloy material friction stir welding. 5083 aluminum alloy offers excellent corrosion resistance, particularly in marine environments, along with good weldability and moderate strength, while 7075 aluminum alloy provides ultra-high strength and hardness for aerospace applications but faces challenges in conventional welding due to the cracking susceptibility. Friction stir welding (FSW) enables defect-free joints with minimal thermal distortion, preserving 5083's corrosion resistance by avoiding HAZ degradation and overcoming 7075's weldability limitations by preventing liquation cracks. This solid-state process makes FSW critical for marine structures using 5083 to maintain the longevity and for aerospace components using 7075 to achieve reliable high-strength welded assemblies.

Therefore, the industrially common 5083 and 7075 aluminum alloys were selected and welded by friction stir welding, and their mechanisms and applications were analyzed, which can provide a theoretical basis and technical support for industrial production.

2 EXPERIMENTAL METHODS

The 5083 aluminum alloy was friction stir welded on a substrate with dimensions of 500 mm × 300 mm × 2.5 mm. The welding process parameters are shown in **Table 1**.

Table 1: Welding process parameters of friction stir welding for 5083 alloy

Sample number	Rotational speed (min ⁻¹)	Travel speed (mm/min)
1–3	600	300
4–6	800	300

The 7075 aluminum alloy was used to make specimens by friction stir welding on a substrate with dimensions of 520 mm × 200 mm × 4 mm. The welding process parameters are shown in **Table 2**.

Table 2: Welding process parameters of friction stir welding for 7075 alloy

Weld seam	Rotational speed (min ⁻¹)	Welding speed (mm/min)
1	1000	200
2	1000	400
3	1200	100
4	1200	200
5	1500	200
6	1500	400

The metallographic structure was observed using a macroscopic microscope (macrostructure) and a Leica metallurgical microscope (microstructure).

The 5083 aluminum alloy was polished electrolytically. The composition of the polishing solution was methanol mixed with perchloric acid (570:60). The parameters of the polishing machine were selected as follows: voltage (U) 17V; polishing time (t) 30s; flow rate (v) 15m/min.

For the macroscopic structure, the etching solution was a mixed acid of H₂O (40 mL) + HNO₃ (30 mL) + HCl (30 mL) + Cu (5g). The specimen was immersed in the etching solution for 20–30s, and then the specimen was quickly taken out and washed clean with absorbent cotton dipped in clean water. If the structure was not obvious, the time could be increased. When the etching time was too long, the specimen would turn black.

After polishing the 7075 aluminum alloy, the specimen was etched. The etching solution for the microstructure was (Keller reagent): a formula of 95 % H₂O, 2.5 % HNO₃, 1.5 % HCl and 1.0 % HF. The method was to immerse the polished surface of the specimen in the pre-prepared etching solution for about 8–10 s. During this period, the specimen should be taken out from time to time to observe the etching degree to prevent over-etching. After etching, the specimen was rinsed with clean water, and then immediately wiped with alcohol-soaked cotton until the weld contour could

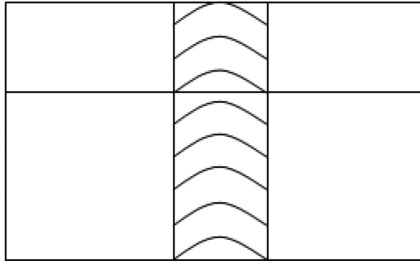


Figure 1: Microhardness measuring position

be clearly seen, and then immediately dried with a hair dryer (cold air). Finally, the specimen required for the experiment was obtained.

Hardness is one of the key indicators of metallic materials. Materials with high strength have stronger resistance to plastic deformation, so their hardness values are also high. The experiment was carried out on a Brinell hardness tester (HB), using a quenched steel ball with a diameter of 1 mm for the indenter. Before the measurement it was necessary to ensure that the upper and lower surfaces of the specimen were parallel to each other to prevent errors in the data. When measuring the hardness, 18 points were measured from the edge to the center on the specimen surface and were kept as straight as possible. To achieve a good balance between the universality (errors caused by different thicknesses of the specimen due to grinding) and the accuracy (errors caused by defects inside the plate and weld) of the measured hardness, each position was tested 5 times, and then the average value was taken. The hardness measurement position is shown in **Figure 1**.

From **Figure 2** it can be seen that under good welding process parameters, the friction stir welded joint of the 5083 aluminum alloy is dense in structure, except for the presence of a keyhole, and there are no visible defects in fusion welding. When the welding process parameters are inappropriate, the tendency of the joint to have flash will become more serious. As can be seen from **Figures 3** and **4**, when the welding speed is constant, the flash will increase with the increase in the rotational speed of the welding tool.

In the FSW process, different regions of the joint are affected by different degrees of heat and stirring. Therefore, the welded joint has different microstructure char-

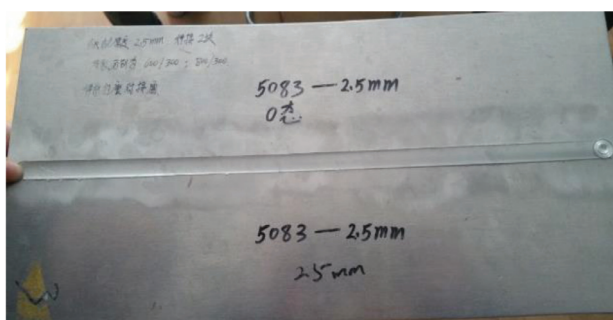


Figure 2: Welding test plate of 5083 aluminum alloy

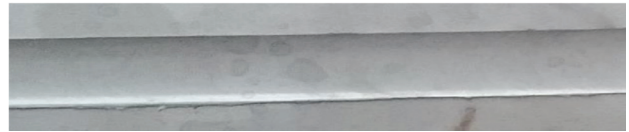


Figure 3: Rotation speed: 600 min^{-1} , welding speed: 300 mm/min



Figure 4: Rotation speed 800 min^{-1} , welding speed 300 mm/min



Figure 5: Microstructure of FSW joint section

acteristics from the traditional fusion welded joint, and the appearance of different parts of the friction-stir-welded joint is also different. As shown in the macroscopic morphology of the FSW joint section in **Figure 5**, the cross-section of the weld joint is divided into four typical parts according to the degree of heat and stirring action on the material. From the base material on both sides to the weld center, they are the base material zone (base material, BM), the heat-affected zone (heat-affected zone, HAZ), the thermo-mechanically affected zone (thermal-mechanically affected zone, TMAZ) and the stirred zone (stir zone, SZ). The macroscopic microstructure of the stirred zone is a trapezoidal (wide at the top and narrow at the bottom) morphology.

In the stirred zone of the FSW joint, a "basin-like" structure that is wide at the top and narrow at the bottom can usually be observed, as shown in **Figures 6a** to **6f**. When the welding speed is 300 mm/min , the "basin-like" structure exhibits different morphologies with the increase in the rotational speed. It shows that the left- and right-hand sides gradually become symmetrical, and the lower end of the weld changes, as shown in **Figures 6c** and **6d**. Continuing to increase the rotational speed, as shown in **Figure 6f**, under the condition of 800 min^{-1} to 300 mm/min , a symmetrical "basin-like" structure with smooth sides on both sides is completed. Regarding the formation of the "basin-like" structure, this is because when the welding speed is constant, by increasing the rotational speed, heat input and stirring degree, the fluidity of the material increases, thus forming a "basin-like" structure with smooth sides and left-right symmetry.

The change in the rotational speed v causes the heat input and stirring degree of the welding joint in the FSW process to change, which is one of the fundamental reasons for the change in the symmetry degree and size of the stirred zone morphology. In the FSW process, the linear energy qE of the joint is expressed as:

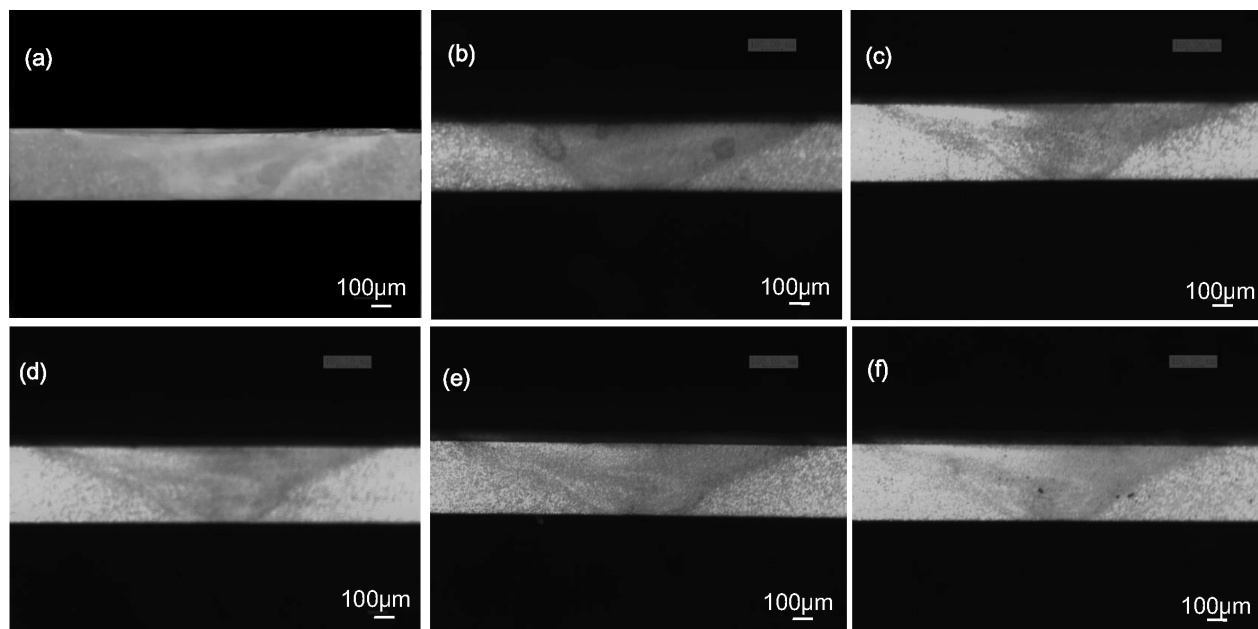


Figure 6: Macro-section of specimen section at each position: a) 600–300 welding starts; b) 600–300 welding is in progress; c) 600–300 lifting rotation speed to 800–300; d) 800–300 welding starts; e) 800–300 welding is in progress; f) 800–300 welding ends

$$q_E = \frac{Q}{v} = k \frac{\mu \omega P}{v} = A \frac{\omega}{v} \quad (1)$$

Where μ is the friction coefficient between the FSW welding tool and the workpiece; ω is the FSW welding tool rotational speed (min^{-1}); P is the pressure on the friction surface; v is the FSW welding speed (mm/min); k is a constant related to the FSW welding tool size. In the formula, the pressure P on the friction surface, the friction coefficient μ and the size-related k are all constants, and their product is a constant A . Therefore, the ratio of the FSW welding tool rotational speed ω and the welding speed v affects the linear energy. In the FSW process, most of the heat entering the material is caused by the friction between the shoulder of the welding tool and the workpiece, and the main function of the welding tool is to stir and help the metal flow. It can be seen from the formula that when the welding speed v is constant, increasing the rotational speed ω of the welding tool, the friction stir welding linear energy q_E increases, the heat input of the joint increases, so that enough metal in the softened state is obtained, and thus the metal fluidity increases. At the same speed, increasing the rotational speed of the welding tool increases the area of the stirred zone. When the welding speed of the welding tool is fixed at 300 min^{-1} , increasing the rotational speed makes the stirred zone left-right symmetrical.

Figure 7 shows the microhardness distribution curves of the alloy at different positions in the welding process with a rotational speed of 600 min^{-1} and a welding speed of 300 mm/min for specimens 1 and 2. It can be seen from the figure that at the beginning of welding, the microhardness peak value in the weld zone is slightly higher than that in the welding process.

When the welding speed is constant (300 mm/min), and the rotational speed is increased to 800 min^{-1} , it can be seen from **Figure 4** that for specimen 3, under the same welding speed, suddenly increasing the rotational speed will cause the microhardness to rise sharply and then gradually decrease and stabilize, as shown in **Figure 8**.

Figure 8 shows the microhardness distribution curves of the alloy at different positions in the welding process with a rotational speed of 800 min^{-1} and a welding speed of 300 mm/min for specimens 5 and 6. It can be seen from the figure that in the welding process, the microhardness peak value in the weld zone is slightly lower than that at the end of the welding. Therefore, the hardness value in the weld zone of the specimen is the high-

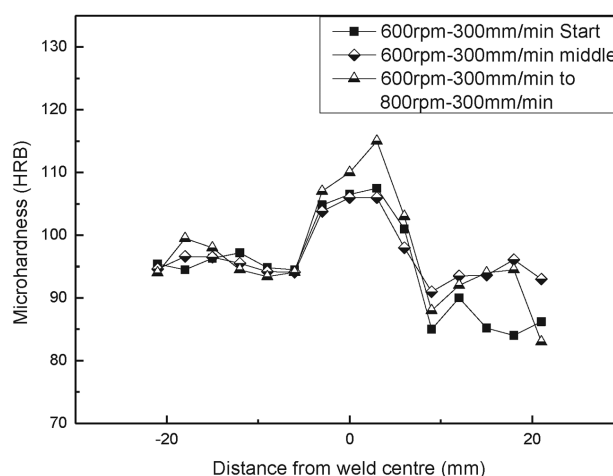


Figure 7: Hardness values at different positions during $600 \text{ min}^{-1} \approx 300 \text{ mm/min}$ welding

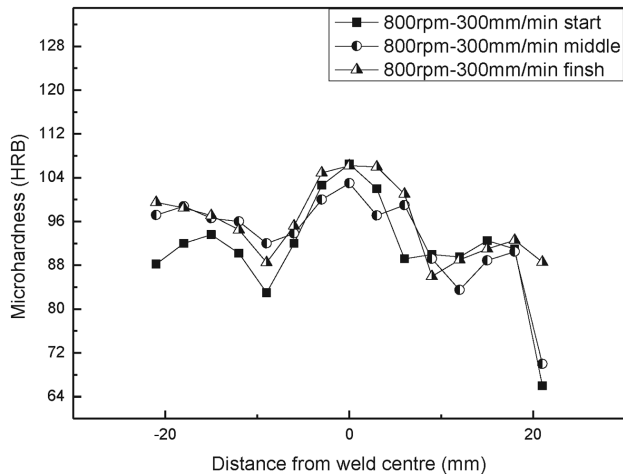


Figure 8: Hardness values at different positions during $800 \text{ min}^{-1} \approx 300 \text{ mm/min}$ welding

est among other parts of the specimen, and specimen 3 has the highest hardness value among all the specimens.

The hardness of the central part of the specimen is higher than that of other parts of the specimen. This is because these regions belong to the weld-nugget zone, and during the welding process, dynamic recrystallization occurs in the grains, and fine equiaxed grains are generated. According to the Hall-Petch formula:

$$\sigma_s = \sigma_0 + Kd^{-\frac{1}{2}} \quad (2)$$

it can be speculated that the fine grains can increase the strength of the weld nugget zone and increase the hardness after strengthening.

When the travel speed is constant, the hardness value in the heat-affected zone gradually decreases with the increase in the rotational speed. This is because when the welding speed is maintained at 300 mm/min , increasing the rotational speed of the welding tool from 600 min^{-1} to 800 min^{-1} causes an increase in heat input, resulting in the growth of dynamically recovered grains. According to the relationship in formula (2), its microhardness value becomes lower.

Research on the microstructure and mechanical properties of the friction-stir-welded joint of 7075 aluminum alloy plate

The welding test of 4-mm-thick 7075-T6 aluminum alloy was carried out by FSW technology. It can be seen

from **Figure 9** that the appearance of the weld after friction stir welding is flat, smooth, symmetrical and good-looking, with good formation. There is no weld protrusion, and the plate has a small amount of deformation after welding.

Table 3 shows the surface morphology of the friction-stir-welded joints of 7075 aluminum alloy under different welding parameters. It can be seen from the table that under the respective welding process parameters, burrs and flashes are visible to the naked eye on both sides of the aluminum-alloy FSW joint. This is because during the welding process, the metal reaches the plastic state due to the extrusion of the shoulder shaft of the welding tool, so burrs and flashes will appear on both sides of the welding tool. It can be seen from the table that on the lower side of the weld, that is, the retreating side, the burrs and flashes are more obvious. Therefore, the difference in the temperature between the advancing side and the retreating side during the welding process will also lead to the difference in the number of burrs and flashes. It can be seen from the table that when ω/v is 2.5 (that is, the rotational speed is 1000 min^{-1} and the welding speed is 400 mm/min), the weld surface is flat and smooth, the arc texture is clear and dense, there are fewer burrs and flashes on both sides of the weld area, the weld deformation is small, and there is no obvious weld protrusion, showing good weld formation. The joint surfaces obtained under other welding parameters are relatively rough (especially welds 5 and 6), with deep friction marks, severe burrs and flashes, and slight peeling.

Figures 10a and **10b** show that the microstructure of the base metal is in a rolled state, and its microstructure is a lath structure along the rolling direction. It can be seen from **Figures 10c** and **10d** that the grains in the heat-affected zone are elongated. This is because during the friction-stir-welding process, the grains are affected by the extrusion of the shoulder shaft of the welding tool and the increase in the temperature around the welding tool, but the degree of grain deformation is not as obvious as that in the weld nugget zone. It can be seen from **Figures 10e** and **10f** that the grains in the weld-nugget zone are uniform and fine, showing an equiaxed shape. This is because under the action of the welding tool, the large grains are broken and then fine grains are generated. Moreover, the temperature around the welding tool

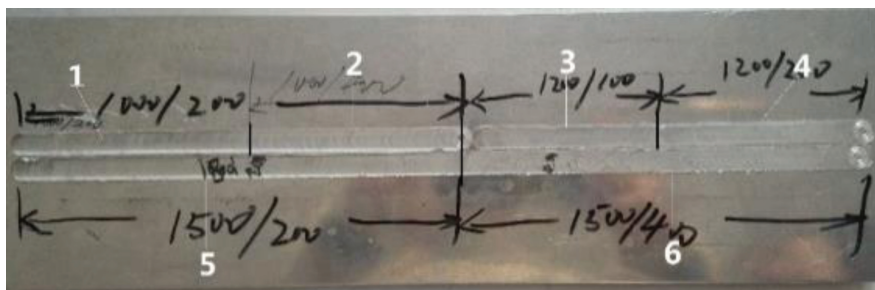



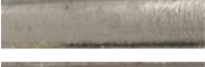




Figure 9: Weld distribution

Table 3: Macro Morphology of Welds

Weld seam	Macrostructure of weld	Welding process parameters	
		Rotational speed (min ⁻¹)	Welding speed (mm/min)
1		1000	200
2		1000	400
3		1200	100
4		1200	200
5		1500	200
6		1500	400

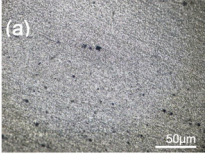
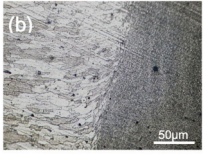
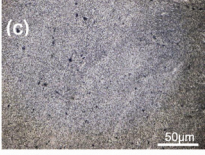
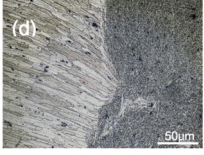
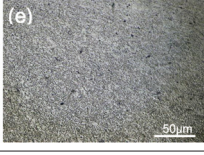
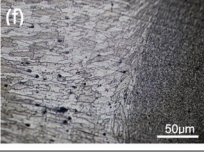
is relatively high, and smaller grains are formed after reaching the recrystallization temperature. The combined action of these two makes the grains in the weld-nugget zone fine.

3 INFLUENCE OF ROTATIONAL SPEED ON THE MICROSTRUCTURE OF THE JOINT

Under different rotational speed parameters, the microstructure of the weld-nugget zone and the thermo-mechanically affected zone of the joint will be affected. It can be seen from **Table 4** that the microstructure presented in the weld-nugget zone is an

equiaxed grain structure, which is fine and uniform. This is because the welding tool causes the grains to break, and the high temperature generated by friction causes the microstructure to undergo dynamic recrystallization, finally forming a fine, equiaxed grain structure.

Table 4: Microstructure of joints at different rotating speeds at welding speed of 200 mm/min

Rotational speed (min ⁻¹)	Weld-nugget zone	Thermo-mechanically affected zone
1000		
		
		

It can also be seen from **Table 4** that when the welding speed is 200 mm/min, under the same welding-speed condition, different rotational speeds of the welding tool have an important impact on the weld area. When the rotational speed of the welding tool is increased from 1000 min⁻¹ to 1500 min⁻¹, the grains in the weld-nugget zone of the joint are fine and uniform at 1000 min⁻¹, and

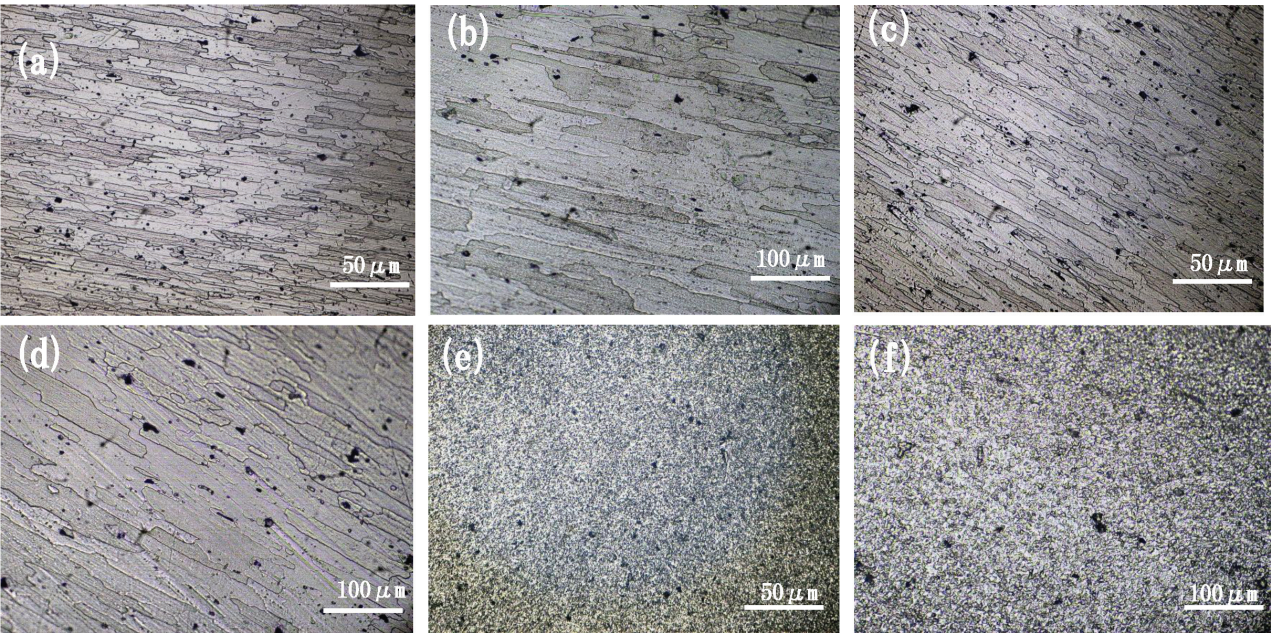


Figure 10: Microstructure of 7075 aluminum alloy friction stir weld (a)–(b) Base metal; (c)–(d) heat affected zone; (e)–(f) nugget zone

the grains in the weld nugget zone become slightly larger when the rotational speed is increased to 1500 min^{-1} . Although it is not obvious, there is a significant difference when compared with the microstructure at other rotational speeds of the welding tool. This is because with the increase in the rotational speed, the temperature in the weld area increases due to the influence of the frictional heat, especially in the weld-nugget zone. Although the welding tool has a crushing effect on the grains in the weld-nugget zone, the higher temperature and more heat in the weld-nugget zone reduce the cooling rate of the metal, resulting in a slight growth of the grains in the weld nugget zone. Moreover, with the increase in the rotational speed, the extrusion of the shoulder shaft of the welding tool on the weld metal causes the surrounding metal to undergo plastic deformation. In addition, with the increase in heat input, the grains in the thermo-mechanically affected zone and the surrounding microstructure also coarsen.

Table 5: Microstructure of joints at different rotating speeds at welding speed of 400 mm/min

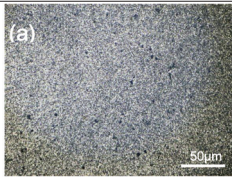
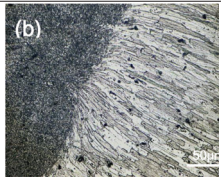
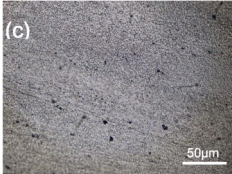
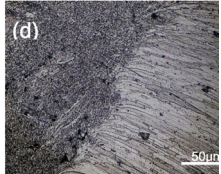
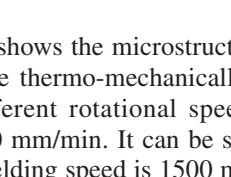
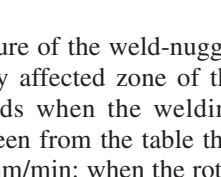
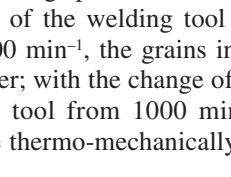
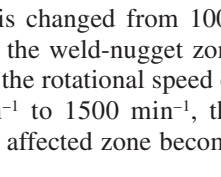
Rotational speed (min^{-1})	Weld-nugget zone		Thermo-mechanically affected zone	
1000	(a)	(b)	(c)	(d)
				
1500	(e)	(f)	(g)	(h)
				

Table 5 shows the microstructure of the weld-nugget zone and the thermo-mechanically affected zone of the joint at different rotational speeds when the welding speed is 400 mm/min . It can be seen from the table that when the welding speed is 1500 mm/min : when the rotational speed of the welding tool is changed from 1000 min^{-1} to 1500 min^{-1} , the grains in the weld-nugget zone become larger; with the change of the rotational speed of the welding tool from 1000 min^{-1} to 1500 min^{-1} , the grains in the thermo-mechanically affected zone become larger.

Figure 11 shows the microhardness distribution curves of the friction-stir-welded joints of 7075 aluminum alloy at different welding speeds when the rotational speed of the welding tool is constant. It can be seen from **Figure 11a** that when the rotational speed of the welding tool is 1200 min^{-1} , and the welding speeds are 100 mm/min and 200 mm/min , respectively, the change in the microhardness in the joint is not significant because the change in the welding speed is not significant enough to have an obvious impact on the microstructure.

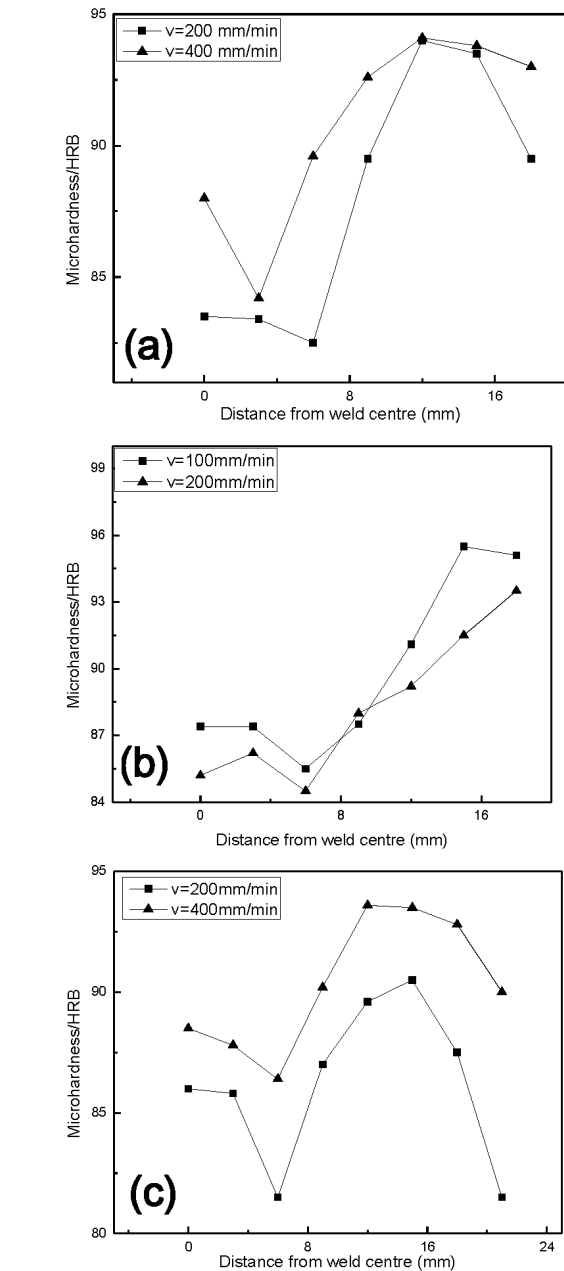


Figure 11: Microhardness distribution at different welding speeds: a) $\omega = 700 \text{ min}^{-1}$; b) $\omega = 1200 \text{ min}^{-1}$; c) $\omega = 1500 \text{ min}^{-1}$

As shown in **Figure 11c**, when the rotational speed of the welding tool is 1500 min^{-1} , and the welding speeds are 200 mm/min and 400 mm/min , respectively, the hardness value of the joint at a welding speed of 400 mm/min is the highest. In addition, it can also be seen from **Figures 11a** and **11c** that the hardness value of the thermo-mechanically affected zone is lower than that of the weld metal. This is because in the vicinity of the thermo-mechanically affected zone, there are partly lath-shaped grains and partly equiaxed grains, resulting in an inhomogeneous microstructure and inconsistent grain size, so the performance is different. The phenomenon

non that the hardness value of the material in the thermo-mechanically affected zone is lower than that in the weld zone occurs. The supply state of the 7075 aluminum alloy used in this experiment is T6 (solution treatment and artificial aging), and the main strengthening mechanism is precipitation strengthening, so a metal material with good mechanical properties is obtained.

4 CONCLUSIONS

In 5083 alloy, higher rotational speeds enhance the "onion ring" symmetry, but increase flash formation, with abrupt speed changes causing weld-center hardness anomalies. For 7075, the rotational speed elevation coarsens NZ/TMAZ grains, while the increased travel speed refines them via thermal-strain modulation.

5083 joints display HAZ grain coarsening and TMAZ transitional structures bridging the BM and NZ equiaxed grains. 7075 exhibits an NZ < BM < TMAZ grain hierarchy, reflecting alloy-dependent dynamic recrystallization responses.

5083 NZ shows peak hardness, whereas 7075 weld metal averages 86.6 HB with TMAZ hardness reduction, both patterns governed by respective grain evolution mechanisms.

Acknowledgements

The authors acknowledge the Study on the mechanical behavior of creep pore nucleation of heat-resistant materials used in the development of dry hot rocks (2021-696).

5 REFERENCES

- ¹ X. Liu, Z. Li, Z. Xu et al., Joint formation and mechanical properties of ultrasonic-assisted transient liquid bonding of dissimilar Al/Mg with a Zn interlayer in air, *Journal of Manufacturing Processes*. 77 (2022) 632–641
- ² S. Ji, S. Niu, J. Liu, Dissimilar Al/Mg alloys friction stir lap welding with Zn foil assisted by ultrasonic, *Journal of Materials Science & Technology*. 35 (2019) 8, 1712–1718
- ³ A. Sharma, V. K. Dwivedi, Y. P. Singh, Effect on ultimate tensile strength on varying rotational speed, plunge depth and welding speed during friction stir welding process of aluminium alloy AA7075, *Materials Today: Proceedings*. 26 (2020) 2055–2057
- ⁴ F. Micari, G. Buffa, S. Pellegrino, L. Fratini, Friction stir welding as an effective alternative technique for light structural alloys mixed joints, *Procedia Engineering*. 81 (2014) 74–83
- ⁵ G. Wu, C. Wang, M. Sun, W. Ding, Recent developments and applications on high performance cast magnesium rare-earth alloys, *Journal of Magnesium and Alloys*. 9 (2021) 1, 1–20
- ⁶ Y. Meng, Y. Lu, Z. Li et al., Effects of beam oscillation on interface layer and mechanical properties of laser-arc hybrid lap welded Al/Mg dissimilar metals, *Intermetallics*, 133 (2021), 107175
- ⁷ K. Singh, G. Singh, H. Singh, Review on friction stir welding of magnesium alloys, *Journal of Magnesium and Alloys*. 6 (2018) 4, 399–416
- ⁸ Bobby Kannan M, Dietzel W, Zeng R et al. A study on the SCC susceptibility of friction stir welded AZ31 Mg sheet[J]. *Materials Science and Engineering A*, 460–461 (2007) 243–250
- ⁹ W. Woo, H. Choo, M. B. Prime et al. Microstructure, texture and residual stress in a friction-stir-processed AZ31B magnesium alloy[J]. *Acta Materialia*, 56 (2008) 1701–1711
- ¹⁰ L. Commin, M. Dumont, J. E. Masse et al. Friction stir welding of AZ31 magnesium alloy rolled sheets: Influence of processing parameters[J]. *Acta Materialia* 57 (2009) 326–334
- ¹¹ N. Afrin, D. L. Chen, X. Cao et al. Microstructure and tensile properties of friction stir welded AZ31B magnesium alloy[J]. *Materials Science and Engineering A* 472 (2008) 179–186
- ¹² U. Suhuddin, S. Mironov, Y. S. Sato et al. Grain structure evolution during friction-stir welding of AZ31 magnesium alloy[J]. *Acta Materialia* 57 (2009) 5406–5418
- ¹³ L. Zhou, H. J. Liu, P. Liu et al. The stir zone microstructure and its formation mechanism in Ti–6Al–4V friction stir welds[J]. *Scripta Materialia* 61 (2009) 596–599
- ¹⁴ L. Liu, Research on the Microstructure and Properties of Friction Stir Welding Joints of 5052/6061 Aluminum Alloy Sheets with the Same Thickness but Different Materials [D]. Wuhan: Master's Dissertation of Hubei University of Technology, 2016